JOURNAL OF MATERIALS SCIENCE 29 (1994) 4913–4917

Formation and hot isostatic pressing of ZrO_2 solid solution in the system ZrO_2–Al_2O_3

S. INAMURA, H. MIYAMOTO
Osaka Prefectural Institute of Industrial Technology, Osaka 550, Japan
Y. IMAIDA, M. TAKAGAWA, K. HIROTA, O. YAMAGUCHI*
Faculty of Engineering, Doshisha University, Kyoto 602, Japan

In the system of ZrO_2–Al_2O_3, cubic ZrO_2 solid solutions containing up to 40 mol% Al_2O_3 crystallize at low temperatures from amorphous materials prepared by the simultaneous hydrolysis of zirconium and aluminium alkoxides. At higher temperatures, they transform into tetragonal solid solutions. Metastable ZrO_2 solid solution powders containing 25 mol% Al_2O_3 have been sintered at 1000–1150 °C under 196 MPa using the hot isostatic pressing technique. The solid solution ceramics consisting of homogeneous microstructure with an average grain size of ≈ 50 nm exhibited a very high fracture toughness of 23 MN $m^{-1.5}$. They have been characterized by X-ray diffraction and electron probe surface analyses.

1. Introduction

Zirconia (ZrO_2) exists in three polymorphic modifications: monoclinic (m), tetragonal (t), and cubic (c). m-ZrO_2 transforms into the tetragonal form at ≈ 1000 °C [1] and then at ≈ 2370 °C into the cubic form having the fluorite-type structure [2]. The high-temperature forms cannot be retained at room temperature because both of these transformations are reversible. However, it has been found that the tetragonal and cubic forms can be stabilized at room temperature by the addition of small amounts of oxides (e.g. MgO, CaO, and certain rare-earth oxides) [3] or by adding Mg_3N_2, Si_3N_4, and AlN [4]. On the other hand, little attention has been given to the formation of ZrO_2 solid solutions in the system ZrO_2–Al_2O_3. Alper [5] published a phase diagram for this system and reported that ZrO_2 solid solutions were formed with up to ≈ 7 mol % Al_2O_3 at 1885 °C. However, Gevales [6] reported no evidence for the formation of solid solutions.

Since the discovery of the transformation toughening of ZrO_2 by Garvie *et al.* [7], many studies have been undertaken to improve the fracture toughness of ceramic materials. Special attention has been paid to partially stabilized ZrO_2. Recent work [8] revealed that the isostatically hot-pressed composites of Y_2O_3–Partially stabilized ZrO_2 and Al_2O_3 gave high fracture toughness and high strength.

In the present study, it was confirmed that metastable ZrO_2 (c- and t-ZrO_2) solid solutions containing up to 40 mol % Al_2O_3 could be prepared at low temperatures from amorphous materials obtained by the simultaneous hydrolysis of zirconium and aluminium alkoxides. Their powders were sintered by using the hot isostatic pressing technique. The present paper deals with the formation and sintering of alkoxy-derived ZrO_2 solid solutions in the system ZrO_2–Al_2O_3.

2. Experimental procedure

Zirconium isopropoxide ($Zr(OC_3H_7)_4$, > 99.9% pure) and aluminium isopropoxide ($Al(OC_3H_7)_3$, > 99.99% pure) were used as-received. The mixed alkoxides were refluxed for 24 h at 82 °C and then hydrolysed by adding aqueous ammonia (28 wt %) at room temperature. The temperature was slowly increased for ≈ 1 h to 75 °C while the resulting suspensions were stirred. The hydrolysis products of the various compositions, shown in Table I, were separated from the suspensions by centrifugation, washed 10 times in hot water, and dried at 120 °C under reduced pressure. (The hydrolysis products of $Al(OC_3H_7)_3$ and $Zr(OC_3H_7)_4$ using aqueous ammonia were gibbsite, $Al(OH)_3$, and an amorphous material, respectively. When the former hydroxide was heated, α-Al_2O_3 was formed at ≈ 1200 °C through intermediate phases. On the other hand, t-ZrO_2 crystallized at 415–440 °C. Therefore, the starting powders were described by the oxide composition.)

Differential thermal analysis (DTA) was conducted in air at a heating rate of 10 °C min^{-1}; α-Al_2O_3 was used as the reference. The starting powders, specimens obtained from the DTA runs after cooling, powders calcined for 1 h at various temperatures and, as will be described, the fraction of the m-ZrO_2 phase for fracture surfaces of test samples, were examined by X-ray diffraction (XRD) using nickel-filtered CuK_α radiation. Interplanar spacings were measured with the aid of an internal standard of high-purity silicon, and

---

*Author to whom all correspondence should be addressed.

0022-2461

unit-cell values were determined by a least-squares refinement. Infrared (i.r.) spectra were taken on specimens which had been pressed into pellets with KBr. Before hot isostatic pressing, the calcined powders were pressed into rectangular blocks at 196 MPa and then isostatically cold-pressed at 392 MPa. The green compacts covered with BN powders were sealed in a Pyrex glass tube under vacuum. Hot isostatic pressing experiments were performed for 1 h at various temperatures under 196 MPa using argon gas as the pressure-transmitting medium. After test samples (4 mm × 35 mm × 3 mm) for measurements were cut from sintered bodies, they were lapped with a SiC disc and then a diamond disc. The bulk densities were verified by the Archimedes method.

3. Results and discussion

3.1 Identification and particle size of starting powder

The starting powders A–I were amorphous. They were highly agglomerated and the primary particle size could not be resolved by scanning electron microscopy (SEM). Examination by transmission electron microscopy (TEM), however, showed primary particles ranging in size from 10–15 nm (Fig. 1). The starting powder, J, contained a small amount of gibbsite ($Al(OH)_3$).

3.2. Crystallization of pure ZrO_2

Fig. 2a shows a DTA curve of powder A; it reveals a sharp exothermic peak resulting from the crystallization of t-ZrO_2 at 415–440 °C. The formation of metastable t- or c-ZrO_2 by various methods, such as thermal decomposition of amorphous hydrous ZrO_2 (e.g. [9]), ball-milling of m-ZrO_2 [10], and hydrothermal treatments of amorphous hydrated ZrO_2 (e.g. [11]) etc., has been reported. In the present study, t-ZrO_2 crystallized when heated at 440 °C after the exothermic peak, and only this form was observed up to 640 °C. Powders heated at ≈ 650 to ≈ 1250 °C were mixtures of t- and m-ZrO_2. The amount of the latter form increased with increasing temperature. Single-phase m-ZrO_2 was produced when heated above 1260 °C. The value of the lattice parameter of t-ZrO_2 obtained by heating for 1 h at 550 °C was $a = 0.5085$ nm and $c = 0.5170$ nm, agreeing with data ($a = 0.509$ nm, $c = 0.518$ nm) [11] of the tetragonal form prepared by the hydrothermal treatment of amorphous hydrated ZrO_2 precipitated from $ZrOCl_2 \cdot 8H_2O$ solution with NH_3.

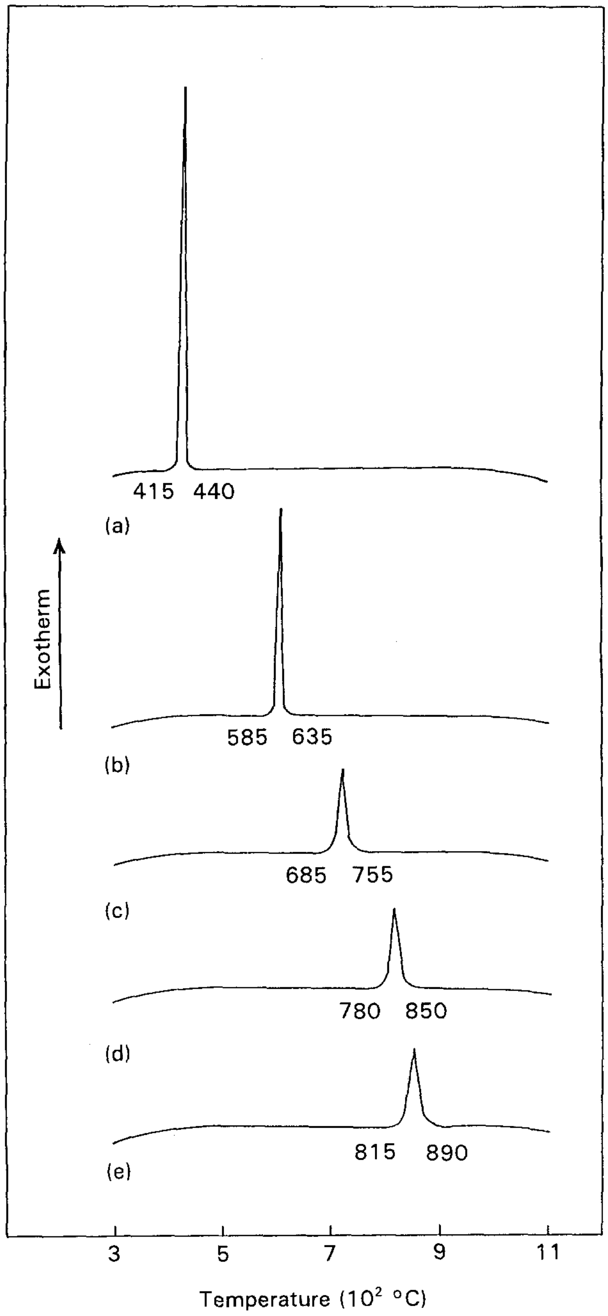

Figure 2 DTA curves for starting powders (a) A, (b) C, (c) E, (d) G, and (e) I.

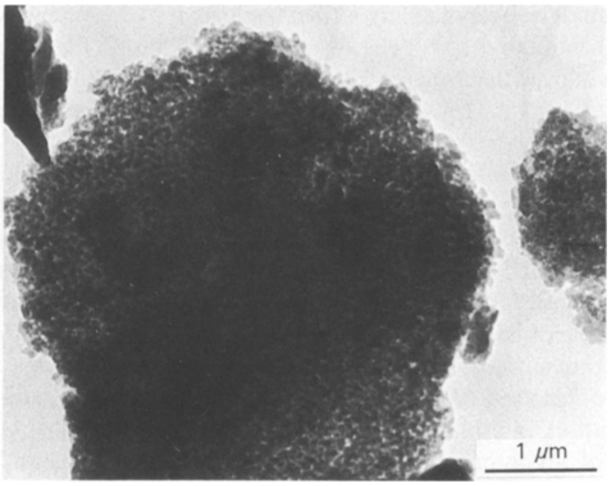

Figure 1 Transmission electron micrographs of starting powder F.

3.3. Crystallization of c-ZrO_2 solid solution

The DTA curves for several starting powders are also shown in Fig. 2. The starting powders B–J showed sharp exothermic peaks. In addition, a small endothermic peak was observed at ≈ 300 °C for J. As will be described, the sharp exothermic peaks were due to the crystallization of c-ZrO_2 solid solutions. Table I

TABLE I Chemical composition of starting powders and crystallization temperature

Starting powder	Composition (mol %)		Crystallization temperature(°C)
	ZrO_2	Al_2O_3	
A	100	0	415–440[a]
B	95	5	535–570
C	90	10	585–635
D	85	15	640–705
E	80	20	685–755
F	75	25	735–805
G	70	30	780–850
H	65	35	805–870
I	60	40	815–890
J	55	45	835–905

[a] Crystallization of tetragonal ZrO_2.

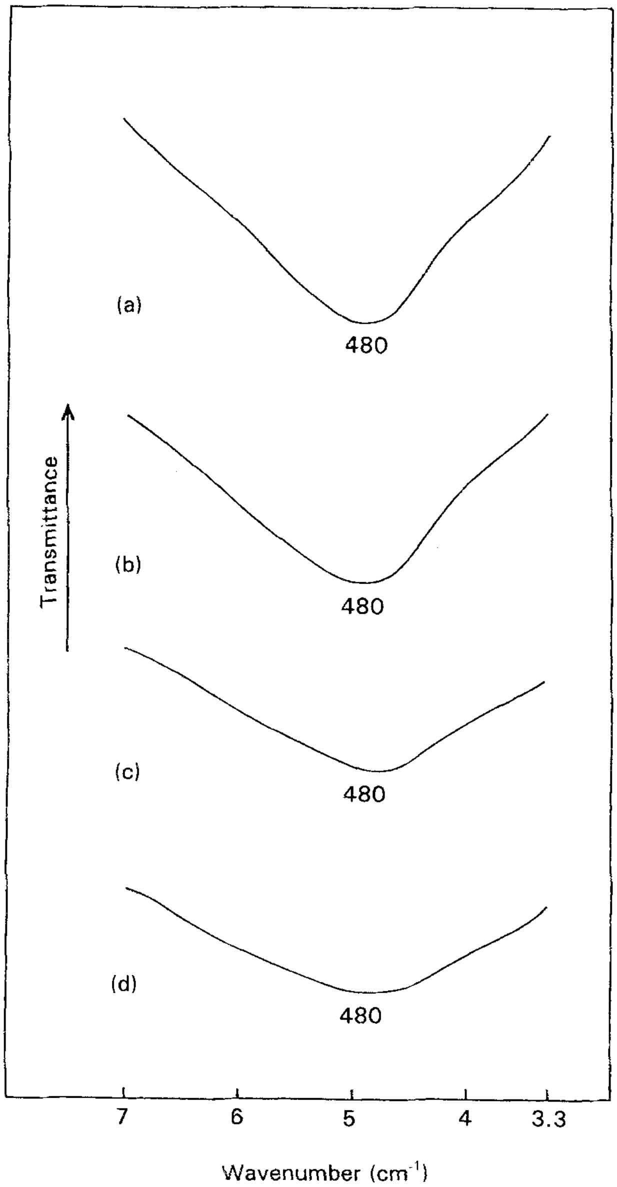

Figure 3 I.r. spectral patterns for c-ZrO_2 phase from starting powders (a) C, (b) E, (c) G, and (d) I.

shows that crystallization occurred at higher temperatures with increasing Al_2O_3 content. Moreover, the peaks decreased successively in height from B–E. However, few changes were observed for F–J. The small endothermic peak in J resulted from the dehydration of gibbsite ($Al(OH)_3$).

No significant change for B–I, being amorphous, was observed up to the temperatures of the sharp exothermic peaks. The specimens heated at temperatures above the DTA peaks were c-ZrO_2 solid solutions containing up to 40 mol % Al_2O_3. Fig. 3 shows the i.r. spectra for c-ZrO_2 solid solutions; these represent the same spectral pattern, although the intensity of the band at ≈ 650 to $\approx 400\ cm^{-1}$ with a centre of $480\ cm^{-1}$ decreased with increasing Al_2O_3 content. The i.r. results also support the formation of c-ZrO_2 solid solutions [12]. Compositional changes result in a significant variation in the cell dimensions. Fig. 4 shows the variation of lattice parameters of the c-ZrO_2 phase; with increasing Al_2O_3 content the lattice parameter a increased linearly from 0.5095 nm to 0.5129 nm. These values were smaller than those of stabilized c-ZrO_2 prepared at high temperatures [13].

3.4. Transformation of c-ZrO_2 solid solution

In relation to the sintering of ZrO_2 solid solution, which will be described in the next section, the transformation of the c-ZrO_2 solid solution from powder F was examined after calcining for 1 h at desired temperatures (Table II). Calcining at 800 and 900 °C yielded c-ZrO_2 solid solutions. t-ZrO_2 solid solutions were formed at 1000 and 1100 °C. The lattice parameter of the t-ZrO_2 solid solution obtained by calcining at 1100 °C was estimated as $a = 0.5119$ nm and $c = 0.5262$ nm; the values were larger than those of

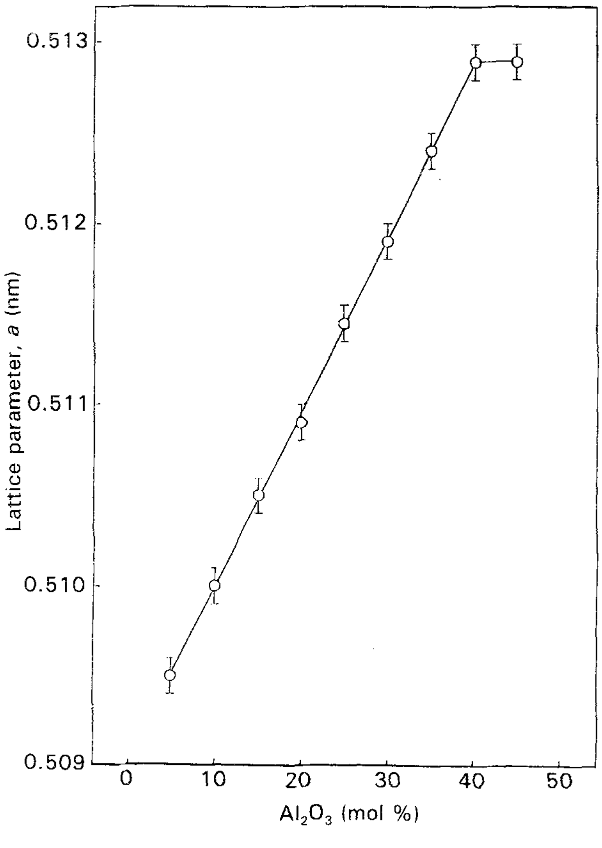

Figure 4 Lattice parameter for c-ZrO_2 phase as a function of composition.

TABLE II Experimental conditions and bulk density, t/m ratio, and mechanical properties of isostatically hot-pressed ZrO_2 solid solution ceramics

Specimen	Calcining temp. (°C)	Phase of calcined powder	HIPing temp. (°C)	Bulk density ($g\,cm^{-3}$)	t/m[a] (%)	K_{IC}[a] ($MN\,m^{-1.5}$)	Bending strength[a] (MPa)
1	800		1000	4.78	70/30	9.5	380
2		Cubic (ss)[b]	1100	5.10	40/60	18	470
3			1125	–	25/75	–	–
4	900		1000	4.75	80/20	11.5	330
5		Cubic (ss)	1100	5.14	55/45	23	570
6			1125	–	35/65	–	–
7	1000		1000	4.98	95/5	4.5	170
8			1100	5.26	70/30	17	700
9		Tetragonal (ss)	1125	5.25	50/50	16.5	470
10			1150	–	30/70	–	–
11	1100	Tetragonal (ss)	1000	4.9	85/15	4.5	130

[a] t/m, K_{IC} and bending strength are average values of three test samples.
[b] ss = solid solution, t = t-ZrO_2, m = m-ZrO_2.

pure t-ZrO_2 described in the preceding section. m-ZrO_2 solid solution having $a = 0.5159$ nm, $b = 0.5242$ nm, $c = 0.5322$ nm, and $\beta = 98.9°$ was produced when calcined at 1200°C. These values, as well as in t-ZrO_2 solid solution, were large in comparison with those of pure m-ZrO_2 data ($a = 0.51463$ nm, $b = 0.52135$ nm, $c = 0.53110$ nm, $\beta = 98.2°$) reported previously [14]. The specimen calcined at 1300 °C was a mixture of pure m-ZrO_2 and α-Al_2O_3.

3.5. Sintering of ZrO_2 solid solution

c- and t-ZrO_2 solid solution powders were prepared by calcining at various temperatures using powder F and sintered by means of hot isostatic pressing. Experimental conditions and results are shown in Table II. The fraction of the m-ZrO_2 phase for test samples was determined from the intensity ratio of the monoclinic $(1\,1\,\bar{1})$ and (1 1 1) lines to the tetragonal (1 1 1) line by XRD analysis [15, 16]. The sintered densities, except for specimen 9 and the fraction of the m-ZrO_2 phase increased with increasing temperature. Visible cracks were recognized in sintered bodies containing the m-ZrO_2 phase above 65 %. No presence of Al_2O_3 in all sintered bodies, as well as in calcined powders, was confirmed. The results suggest that metastable ZrO_2 solid solution ceramics could be prepared. The fracture toughness was evaluated by the microindentation technique. A load of 490 N was applied to the samples, and K_{IC} values were calculated using the equation reported by Niihara *et al.* [17]. As shown in Table II, specimen 5 gave the maximum fracture toughness of 23 $MN\,m^{-1.5}$. It is considered that the fracture toughness obtained from the present method is related to crack propagation. Therefore, the results indicate that a large amount of stress-induced transformation led to a higher value of K_{IC}. SEM was utilized for the microstructural observations. The texture consisted of homogeneous microstructure with an average grain size of ≈ 50 nm (Fig. 5). No ZrO_2 ceramics consisting of nanometre grain size have ever been reported in the literature. The sintered bodies after indentation were examined by electron probe surface analyser. A few micrometres of "upheaval" resulting from plastic deformation were observed in the indented surroundings (Fig. 6). Three-point bending strength was measured using a 30 mm span and a crosshead speed of 0.5 mm min^{-1}. The highest value was 700 MPa for specimen 8 (Table II). The present strength was weak in comparison with that of the isostatically hot-pressed (for 0.5 h at 1500 °C and 100 MPa) composites of Y_2O_3–partially stabilized ZrO_2 and Al_2O_3 [8]. From the above results, metastable ZrO_2 solid solution ceramics in the system ZrO_2–Al_2O_3 were found to give very high fracture toughness. In this connection, it would be interesting to study the improvement of the strength in this ceramic.

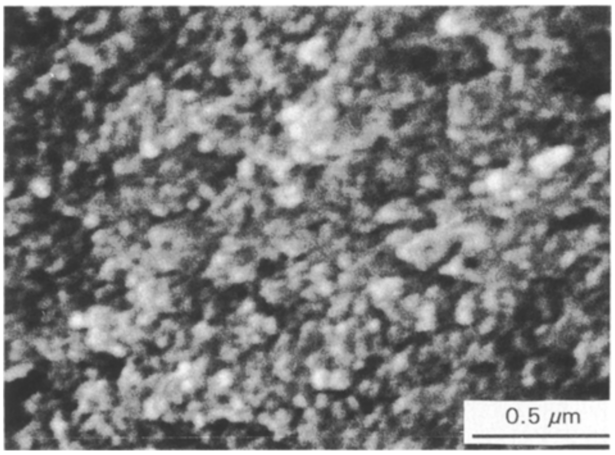

Figure 5 Scanning electron micrograph of specimen 5.

4. Conclusion

In the system ZrO_2–Al_2O_3, metastable ZrO_2 solid solutions containing up to 40 mol % Al_2O_3 are formed from amorphous materials prepared by the simultaneous hydrolysis of zirconium and aluminium alkoxides. The composition 75 mol % ZrO_2–25 mol % Al_2O_3 powders have been sintered using the

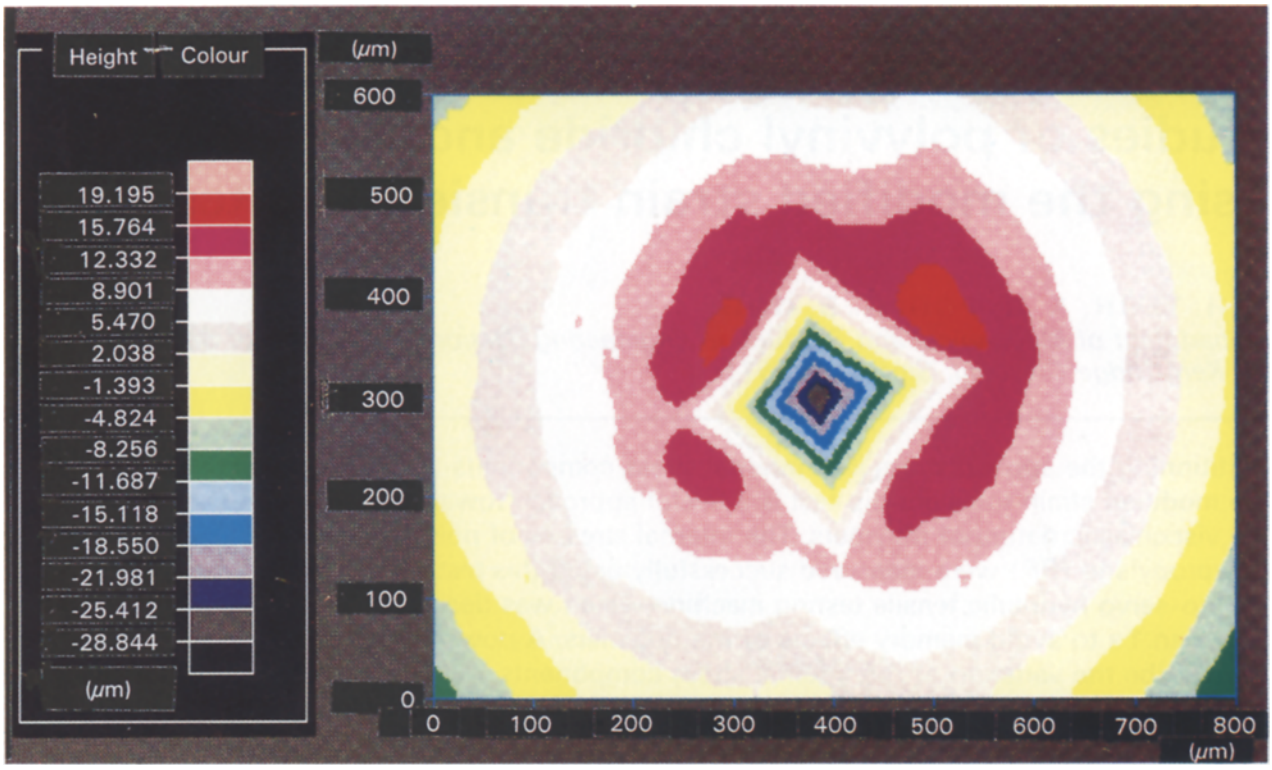

Figure 6 Electron probe surface analysis of specimen 5.

hot isostatic pressing technique. The solid solution ceramics consisting of nanometre grain size give very high fracture toughness of 23 MN m$^{-1.5}$

References

1. G. TEUFER, *Acta Crystallogr.* **15** (1962) 1187.
2. D. K. SMITH and C. F. CLINE, *J. Am. Ceram. Soc.* **45** (1962) 249.
3. L. H. SCHOENLEIN, L. W. HOBBS and A. H. HEUER, *Acta Crystallogr.* **13** (1980) 375.
4. N. CLAUSSEN, R. WAGNER, L. J. GAUCKLER and G. PETZON, *J. Am. Ceram. Soc.* **61** (1978) 369.
5. A. M. ALPER, in "Science of Ceramics", Vol. 3, edited by G. H. Stewart (Academic Press, London, 1967) p. 339.
6. G. GEVALES, *Ber. Dtsch. Keram. Ges.* **45** (1968) 216.
7. R. C. GARVIE, P. H. J. HANNINK and R. T. PASCOE, *Nature* (*Lond.*) **258** (1975) 703.
8. K. TSUKUMA, K. UEDA and M. SHIMADA, *J. Am. Ceram. Soc.* **68** (1985) C-4.
9. T. MITSUHASHI, M. ICHIHARA and U. TATSUKE, *ibid.* **57** (1974) 97.
10. J. E. BAILEY, D. LEWIS, Z. M. LIBRANT and L. J. PORTER, *Trans. J. Br. Ceram. Soc.* **71** (1972) 25.
11. H. NISHIZAWA, N. YAMASAKI, K. MATSUOKA and H. MITSUSHIO, *J. Am. Ceram. Soc.* **65** (1982) 343.
12. K. S. MAZDIYASNI, C. T. LYMCH and J. S. SMITH, *ibid.* **50** (1967) 532.
13. G. KATZ, *J. Am. Ceram. Soc.* **54** (1971) 331.
14. Powder Diffraction File, Card No. 13-307. Joint Committee on powder Diffraction Standards, Swarthmore, PA (1972).
15. R. C. GARVIE and P. S. NICOLSON, *J. Am. Ceram. Soc.* **55** (1972) 303.
16. H. TORAYA, M. YOSHIMURA and S. SOMIYA, *ibid.* **67** (1989) C-119.
17. K. NIIHARA, R. MORENA and D. P. H. HASSELMAN, *J. Mater. Sci. Lett.* **1** (1982) 13.

Received 2 June 1992
and accepted 11 January 1993